Optimizing Circular Arrays with Concentric Subarray Rings for Wireless Power Transmission Applications

Jafar Ramadhan Mohammed

Ninevah University, Mosul, Iraq

https://doi.org/10.26636/jtit.2026.1.2387

Abstract — The emerging wireless power transmission technology creates new opportunities in numerous real-world applications such as wireless charging systems, robots, and aerospace solutions. This paper introduces an optimized method for designing transmit antenna arrays which may be used for long-distance wireless power transmission with narrow focusing of RF power on remote receivers. The novelty of this paper consists in using an effective clustered subarray rings configuration with a transmit circular array instead of its conventional full aperture array, based on the configuration of individual elements. The final goal is to obtain simpler, cheaper, and lighter arrays. Amplitude and phase excitation weighting as well as the number of elements in each clustered subarray are optimized jointly to maximize the efficiency of transferring power to a target region while minimizing sidelobe powers outside the intended region. The simulation results show that the beam collection efficiency of the proposed system with 21 subarray rings was 98.99%, while that of the conventional circular array with individual dense elements of size 21×21 equaled 99.68%.

Keywords — beam collection efficiency, circular array, concentric ring subarrays, wireless power transmission

1. Introduction

Wireless power transmission (WPT) is a system that inverts electrical power into microwave power and transmits it through a wireless channel. Array antennas are used to transmit microwave powers to the intended regions [1]. At the receiving site, rectifier antennas are used to capture microwave powers and reconvert them back into electrical power in order to feed the target receiver devices [2], [3].

Real-life applications of long-distance WPT include charging systems for electric vehicles and electronic devices such as smartphones, smartwatches, and biomedical devices, including those that can be implanted in the human body. The technology may be also used in drone-based RFID systems for monitoring living organisms and may be relied upon in the aerospace industry for transferring power between spacecraft. Industrial robots and automated systems are common use cases of this technology as well [4], [5].

Phased arrays are deployed in WPT to highly efficiently concentrate RF power delivered to remote receivers while minimizing sidelobe powers present outside the intended receivers [6]–[10]. High efficiency, narrow focused arrays require numerous radiating elements, and the resulting arrays with a highly dense arrangement are capable of achieving excellent power transmission efficiency and range. However, these large-scale arrays often face critical challenges such as high cost, high power consumption, and increased hardware complexity [11]–[15]. These drawbacks are proportional to the number of elements in the array or the size of the entire array. This renders the hardware impractical.

In contrast, clustered subarray designs offer significant advantages, such as cost reduction, lower power consumption, and reduced hardware complexity, as their array elements are grouped into specific categories [16]–[19]. Each cluster shares a common amplitude and phase excitation weighting mechanism. Therefore, its array feeding network is much simpler, lighter, and consumes less power – with all those design parameters being of high significance when deploying these transmit arrays in limited space systems, such as drones [20]–[22]. Although clustered arrays provide near-optimal solutions with a smaller number of design parameters, it meets better hardware constraints.

The most important performance metric used to evaluate WPT systems is beam collection efficiency (BCE) – a parameter which may be defined as the ratio of the received power from the rectifying antenna to the total transmitted power [23]. Small size arrays with fewer radiating elements are not capable of achieving the required BCE values. Therefore, larger arrays with dense element arrangements are generally used in these applications.

One of the effective approaches to implement such large-scale arrays relies on clustered subarray configurations [24]–[26]. Clustered subarrays are practically more efficient than fully dense element arrangements. Thus, only a small number of clusters is needed to meet the required BCE values. The works described in [26], [27] presented an optimization algorithm used to generate clustered subarrays, while in [28]–[30], clustered rings were used to design rectangular planar arrays. The design of circular planar arrays with concentric subarray rings is a new idea and can offer a great advantage when it comes to modern wireless communication system applications. The idea is to effectively approximate amplitude excitation weights of the fully circular array elements by using a set of concentric subarray rings starting from the largest (or outer) ring at the array's perimeter and ending at

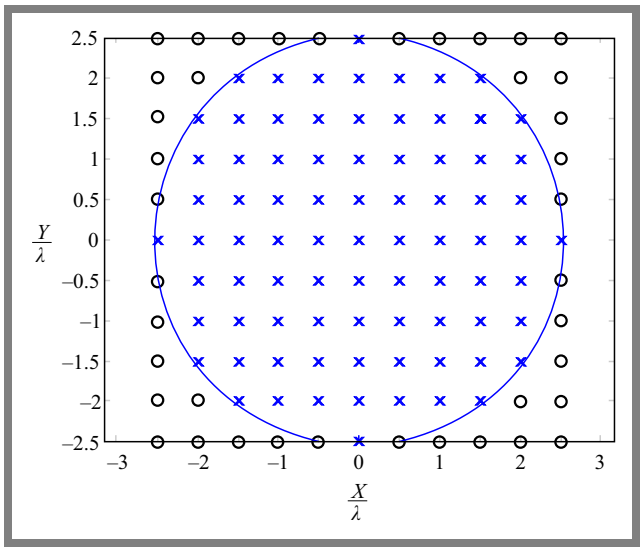

Fig. 1. Geometry of the circular planar array.

the center of the array – in a manner resembling the shape of a circular, ascending ladder.

This new configuration of clustered rings is presented in this paper for the very first time. Once the concentric subarray rings have been created, their amplitude and phase distributions are optimized to maximize the efficiency of transferring power to a target region while minimizing sidelobe powers outside the intended region.

To improve the BCE of the wireless power transmission system, a hybrid optimization algorithm is used in the clustered rings configuration, where the genetic algorithm and the k-means clustering approach are used.

Implementation of the proposed clustered level array instead of its conventional element-based counterpart offers many advantages, such as simplified feeding network, efficient taper efficiency, lower side lobe level, and higher directivity.

2. Circular Array Based on Individual Elements

A circular array with N individual elements is formed by considering a regular square-grid array element with a circular boundary at the array ends, as shown in Fig. 1.

The corner elements that are located outside the circular boundary are turned off, while all the remaining elements that are located inside the circular boundary are active and are assumed to be isotropic. The element pattern and the mutual coupling effect between the active elements are neglected, and thus the array factor with such a configuration can be given by:

$$AF(u,v) = \sum_{n=1}^{N} w_n e^{j[k(ux_n+vy_n)]} , \tag{1}$$

where $w_n = Amp_n\, e^{jPh_n}$ is the element excitation weight in terms of amplitude Amp_n and phase Ph_n of the n-th element, x_n, y_n is the element's location along the x and y axes, $k = \frac{2\pi}{\lambda}$, λ is the wavelength, $u = \sin\theta\cos\varphi$, $v = \sin\theta\sin\varphi$ are the angular coordinates, θ and φ are the elevation and azimuth angles, respectively.

The beam collection efficiency (BCE) metric is defined as the ratio of the received power at the rectifying antenna to the total transmitted power:

$$BCE = \frac{P_R}{P_T} = \frac{\int_{\psi} |AF(u,v)|^2 \,\mathrm{d}u\,\mathrm{d}v}{\int_{\phi} |AF(u,v)|^2 \,\mathrm{d}u\,\mathrm{d}v} , \tag{2}$$

where ψ and ϕ are the fields of view for the received and transmitted powers, respectively.

For a rectangular grid array, the range of either ψ or ϕ can be represented by:

$$\psi = \left\{(u,v) : -u_0 \leqslant u \leqslant u_0,\ -v_0 \leqslant v \leqslant v_0,\right\} . \tag{3}$$

Thus, the denominator of Eq. (2) can be expressed as:

$$P_R = \int_{-u_0}^{u_0}\int_{-v_0}^{v_0} e^{jk(x_m u+vy_m)} e^{-jk(x_n u+vy_n)} \mathrm{d}u\,\mathrm{d}v . \tag{4}$$

$AF(u,v)$ can be found in terms of the element excitation weights w_n^e of the array elements and the steering vector $\boldsymbol{V}(u,v)$, in the following manner:

$$AF(u,v) = \boldsymbol{w}^H \boldsymbol{V}(u,v) , \tag{5}$$

where:

$$\boldsymbol{w} = [w_1^e\, w_2^e \ldots w_N^e]^H,\ n = 1,2,\ldots,N ,$$

$$\boldsymbol{V}(u,v) = \left[e^{-jk(x_1u+vy_1)}\, e^{-jk(x_2u+vy_2)} \ldots\, e^{-jk(x_Nu+vy_N)}\right]^H ,$$

and H is the conjugate transpose. Now, substituting Eq. (3) in Eq. (2), BCE for the circular planar array based on the individual element configuration can be rewritten as:

$$BCE = \frac{\boldsymbol{w}^H\{\int_{\psi} \boldsymbol{V}(u,v)\boldsymbol{V}^H(u,v)\,\mathrm{d}u\,\mathrm{d}v\}\boldsymbol{w}}{\boldsymbol{w}^H\{\int_{\phi} \boldsymbol{V}(u,v)\boldsymbol{V}^H(u,v)\,\mathrm{d}u\,\mathrm{d}v\}\boldsymbol{w}} . \tag{6}$$

3. Circular Array Based on Concentric Subarray Rings

The circular array based on the dense element arrangements that was shown in the previous section is now divided into several concentric subarray rings or clusters equal to C, as shown in Fig. 2. The number of cluster rings is always less than the total number of the individual elements, i.e. $C < N$. The individual elements and the clustered subarray rings of the circular array are related by a matrix with dimension $N \times C$, as follows:

$$M = \begin{bmatrix} M_{11} & \ldots & M_{1C} \\ \vdots & \vdots & \vdots \\ M_{N1} & \ldots & M_{NC} \end{bmatrix} , \tag{7}$$

where

$$M_{nc} = \begin{cases} 1 \text{ if } n\text{-th element belongs to } c\text{-th cluster} \\ 0 \text{ if } n\text{-th element does not belong to } c\text{-th cluster.} \end{cases} \tag{8}$$

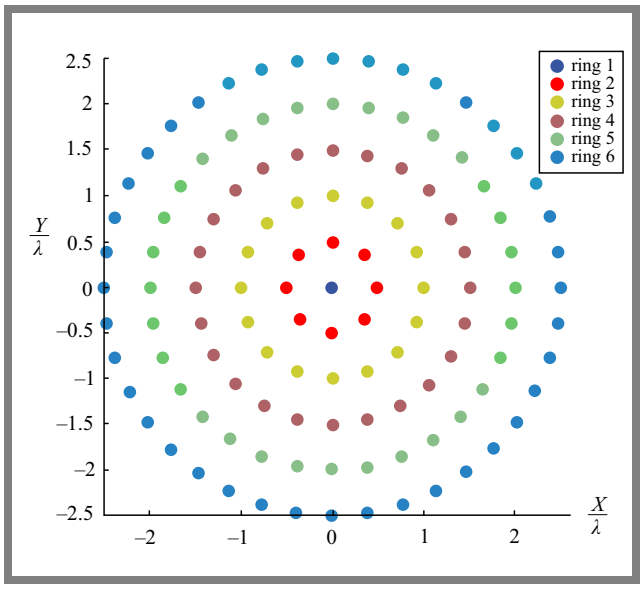

Fig. 2. Geometry of the proposed circular array with concentric subarray rings.

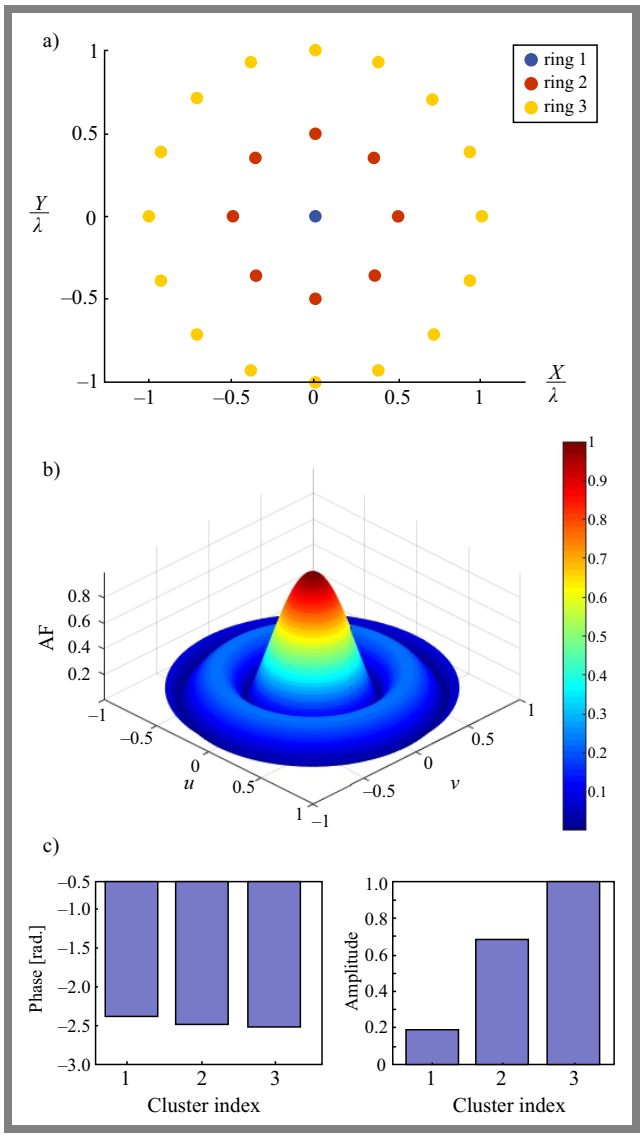

Fig. 3. Results for concentric subarray rings for $C = 3$.

The excitation weights of the resulting cluster rings can be presented by a vector of dimension $C \times 1$ as $\boldsymbol{w}^c = [w_1^c\ w_2^c\ \ldots\ w_C^c]^H$. Then, the excitation weights of each element in the clustered array can be written as:

$$\boldsymbol{w}_{new} = \boldsymbol{M}\,\boldsymbol{w}^c\,. \tag{9}$$

The beam-collecting efficiency of the circular array based on concentric subarray rings can be given by:

$$BCE_{rings} = \frac{\boldsymbol{w}_{new}^H \left\{ \int_\psi \boldsymbol{V}(u,v)\boldsymbol{V}^H(u,v)\,\mathrm{d}u\,\mathrm{d}v \right\} \boldsymbol{w}_{new}}{\boldsymbol{w}_{new}^H \left\{ \int_\phi \boldsymbol{V}(u,v)\boldsymbol{V}^H(u,v)\,\mathrm{d}u\,\mathrm{d}v \right\} \boldsymbol{w}_{new}}\,. \tag{10}$$

The fields of view of the transmitting ϕ, and receiving ψ arrays were of the rectangular geometry, as given by Eq. (3). Here, the fields of view are extended to descript the circular target region as follows:

$$\psi = \left\{ (u,v) : \sqrt{u^2+v^2} \leqslant r_0 \leqslant \sin\theta_o \right\}. \tag{11}$$

Where r_0 represents the radius of the circular aperture and θ_0 is the main beam direction of the pattern. The denominator of Eq. (10) can be expressed as:

$$P_R = \int_0^{\theta_0} \int_0^{2\pi} e^{jk(x_m+y_m)\sin\theta\cos\phi} e^{-jk(x_n+y_n)\sin\theta\sin\phi} \mathrm{d}\phi \sin\theta \mathrm{d}\theta\,. \tag{12}$$

From Eqs. (4) and (12), it was shown that beam collection efficiency is a function of the design variables of the excitation weights at the element level, i.e. w^e for the ordinary circular array without subarray rings, or of the excitation weights at the subarray level, i.e. w^c for the circular array based on clustered subarray rings. A circular planar array with concentric subarray rings is considered here and each ring represents a single cluster. The following steps are used to find the excitation weights of the clustered subarray rings w^c [31].

Starting from the central element of the array, the first clustered weight w_1^c is calculated as $w_1^c = \frac{w_i^e + w_j^e}{2}$, where $i, j = 1, 2, \ldots, N$, $i \neq j$, w_i^e and w_j^e are the element excitation weights of two elements that have the smallest distance equal to $|w_i^e - w_j^e|$. Then, the second clustered weight w_2^c is computed from the largest distance between remaining element excitation weights and the first cluster weight, i.e., $w_2^c = \max\{d(w_i^e, w_1^c)\}$. The third clustered weight w_3^c, is derived from the smallest distance from w_1^c and w_2^c as:

$$w_3^c = \max\left\{ \min\{d(w_i^e, w_1^c), d(w_i^e, w_2^c)\} \right\}.$$

The remaining clustered excitation weights are computed as follows:

$$w_k^c = \max\left\{ \min\{d(w_i^e, w_1^c), d(w_i^e, w_2^c), \ldots, d(w_i^e, w_C^c)\} \right\}$$
$$k = 1, 2, \ldots, C\,, \tag{13}$$

where C is the total number of cluster rings.

To obtain better results, these clustered excitation weights are considered initial values for the optimized algorithm. A genetic algorithm with the following cost function was used

to maximize beam collection efficiency:

$$F\{w_1^c, w_2^c, \ldots, w_C^c, N_1^c, N_2^c, \ldots, N_C^c\} = -BCE$$
$$\text{s.t. } 0 < w_k^c \leqslant 1 \text{ and } 1 \leqslant N_k^c \leqslant N - C+ \tag{14}$$

where N_k^c is the number of array elements in each clustered subarray ring $k = 1, 2, \ldots, C$.

4. Simulation Results

In order to illustrate the effectiveness of the proposed circular array with concentric subarray rings for wireless power transmission, extensive simulation results are presented below:

In all considered examples, the distance between transmitter and receiver sites is assumed to be 100 m and the target region is limited by the angular separation of $\pm 3^\circ$ on both sides of the broadside direction, along both elevation and azimuth planes. The transmitting power is assumed to be 1 W. The radial spacing between any two successive subarray rings is 0.5λ. For genetic optimization, we used the built-in function called `fmincon` with the maximum number of iterations equal to 400.

In the first example, the circular radius of the transmitting circular array is $R_t = 1.0\lambda$, i.e., the number of the circular subarray rings is $C = 3$, including the central element of the array. For this case, the normalized transmitted and received power values are 1 and 0.8486, respectively, while the beam collection efficiency is BCE $= 84.59\%$. The geometrical configuration of the resulting circular array with 3 concentric cluster rings, its corresponding far-field radiation pattern as well as their subarray amplitude and phase excitation weights are shown in Fig. 3.

The normalized received power variations in both RF and DC values, as a function of the target angular region bounded by $\pm 3^\circ$, is shown in Fig. 4. For comparison purposes, the results of the circular array based on individual elements are depicted in Fig. 5.

From the figures presenting the array geometries (compare Fig. 3a with Fig. 5a), it is clear that the array feeding network in the proposed arrangement with circular subarray rings is less complex. Also, from figures of radiation patterns (Fig. 3b with Fig. 5b), it becomes clear that the pattern of the proposed circular subarray rings is almost like that of the conventional array with dense element arrangements and feeding RF components.

In the second example, the design of circular clustered subarrays with different numbers of rings was studied. The results are shown in Figs. 6–8. It is obvious from those results that the concentration of radiation patterns improves along with an increase in the number of concentric subarray rings. On the other hand, array geometries are becoming more complicated.

In the next example, the design of the array feeding structure is considered, where the number of concentric subarray rings equaled 6, including the central element. Figure 9 shows the geometric layout of the designed feeding network for the circular array with concentric subarray rings.

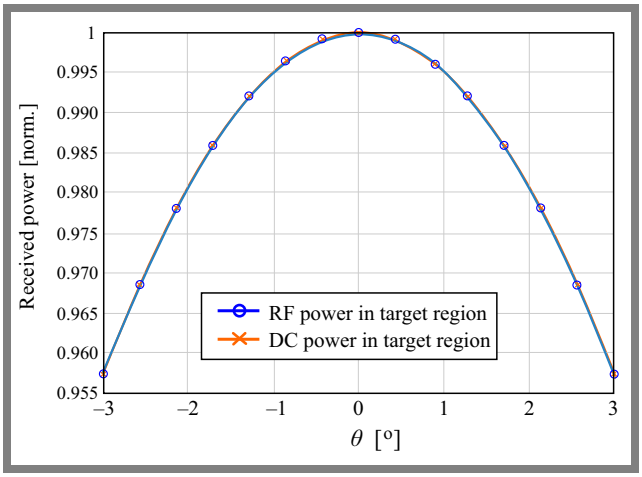

Fig. 4. Variations in received power versus target region for $C = 3$.

Tab. 1. Beam collection efficiencies for various subarray rings.

Method	Normalized P_T	Normalized P_R	BCE [%]
Circular array based on individual elements	1	0.996	99.68
Circular array with 3 subarray rings	1	0.848	84.86
Circular array with 6 subarray rings	1	0.870	87.01
Circular array with 10 subarray rings	1	0.945	94.54
Circular array with 21 subarray rings	1	0.989	98.99

The number of transmitting elements in the first cluster ring amounted to 8, while the number of other rings equaled 16, 24, 32, and 40. Since all transmitting elements that belong to a certain ring share a common amplitude and phase, the required number of amplitude and phase weightings (i.e., the number of RF attenuators and phase shifters) is equal to the number of subarray clustered rings $C = 6$.

From Fig. 9, the central individual element is left without being connected to any attenuators or phase shifters, since its normalized amplitude weighting is one while its phase is zero. The proposed circular subarray rings require only 5 RF attenuators and 5 phase shifters, whereas a conventional circular array based on individual element arrangements needs 140 RF attenuators and 140 phase shifters. This great reduction makes the proposed circular array lighter, lowers its power consumption, renders simpler, and cheaper.

Table 1 shows the variations of the beam collection efficiencies versus the number of clustered subarray rings. BCE improves as the number of subarray rings increases.

From this table, one may notice that BCE of the ordinary circular matrix with individual elements of size 21×21 is better than the results from the proposed matrix with a certain number of sub-array rings. However, the difference between these two values vanishes for a larger number of subarray rings.

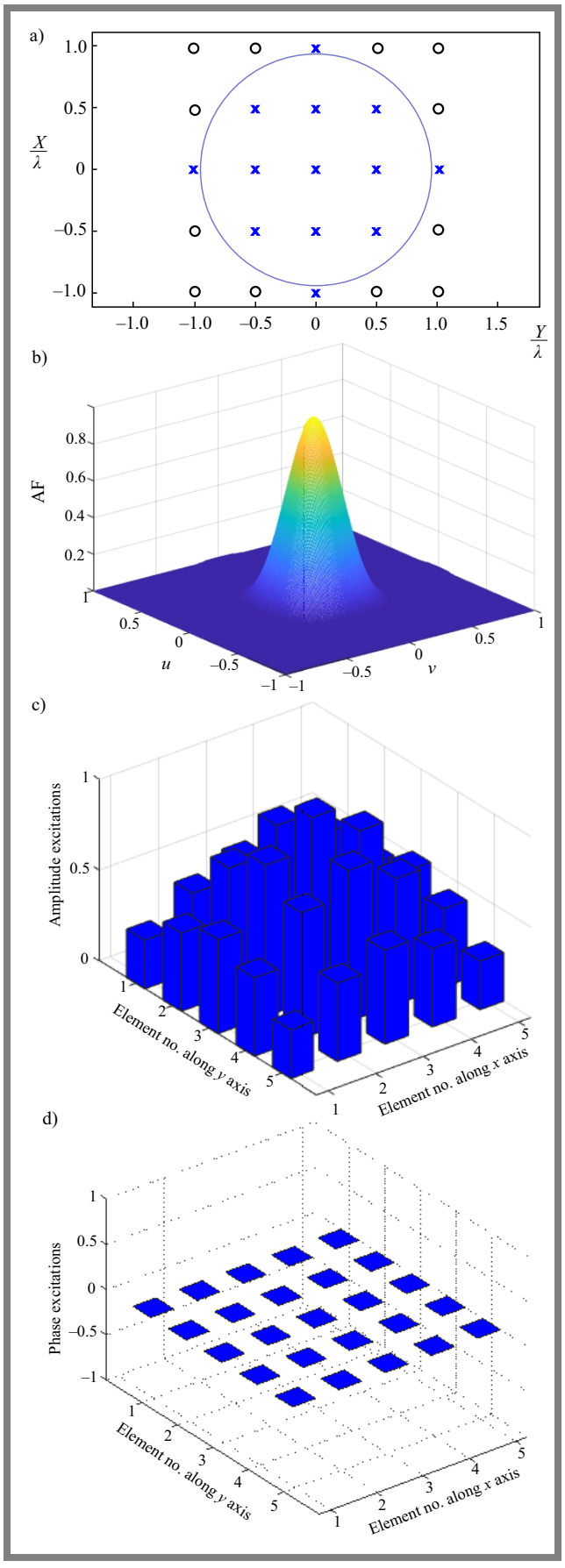

Fig. 5. Results for the conventional circular array with individual elements of size 5×5.

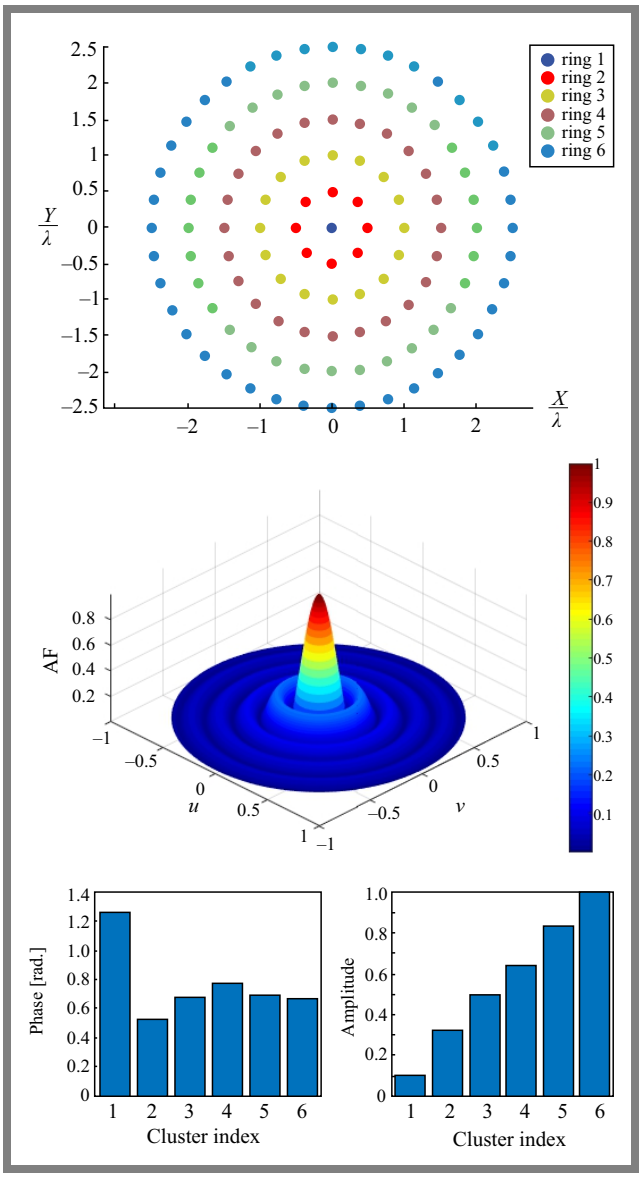

Fig. 6. Results for concentric subarray rings for $C = 6$.

5. Conclusions

A circular planar array with concentric subarray rings was proposed as a simpler alternative to conventional fully dense array elements in order to improve beam collection efficiency while simultaneously significantly reducing the number of hardware components making up the array feeding network Thus, the designed array becomes lighter and consumes less power, which is very important in applications that require long-term operation with limited resources and space.

A k-means clustering approach was adopted and optimization of the genetic algorithm was performed to optimize the design parameters of the proposed concentric subarray rings (i.e., amplitude and phase excitation weights of the subarray rings, number of rings, and the total number of elements in each separate ring), in order to maximize beam collection efficiency.

From the results, it was shown that BCE, radiation pattern, array structure, and feeding network complexity of the proposed

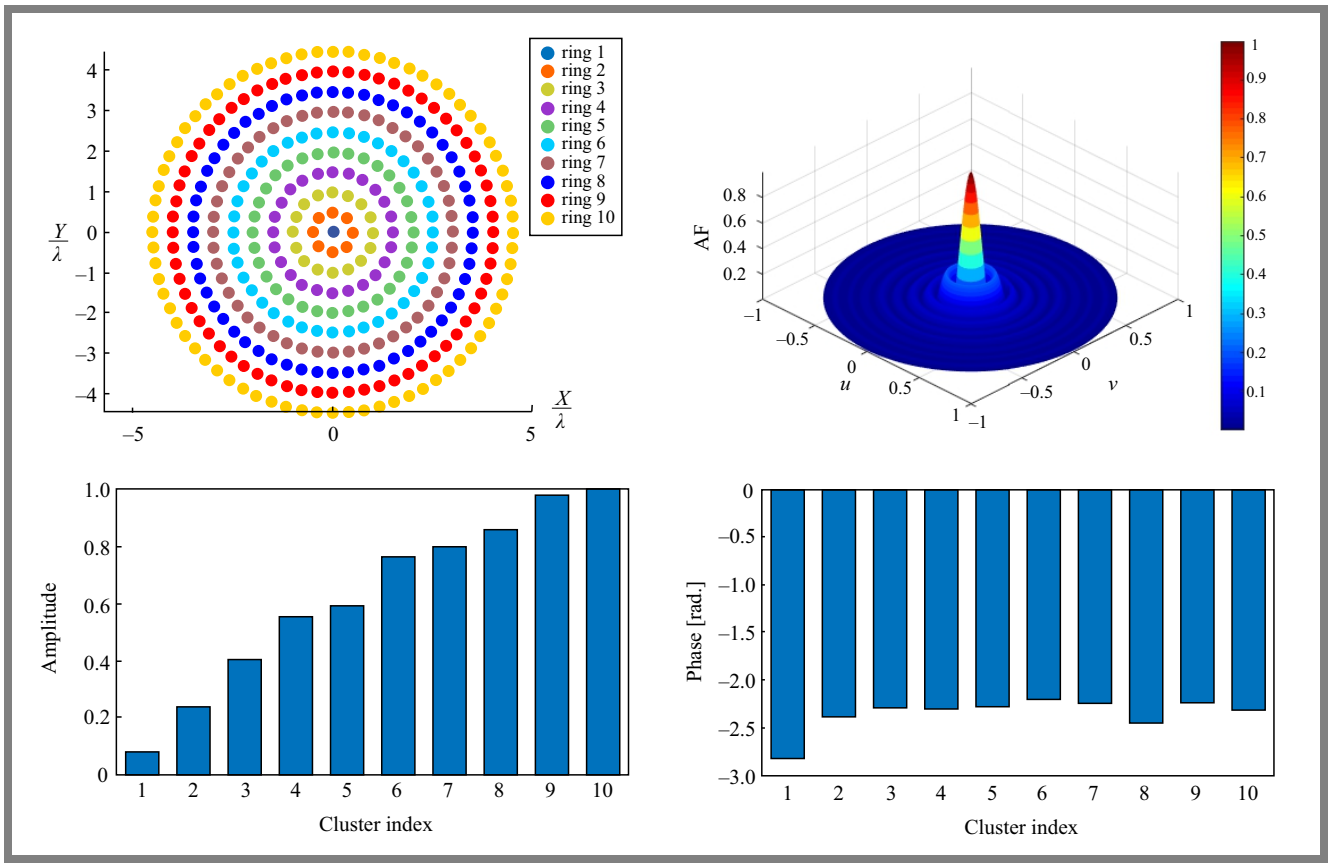

Fig. 7. Results for the proposed antenna for $C = 10$.

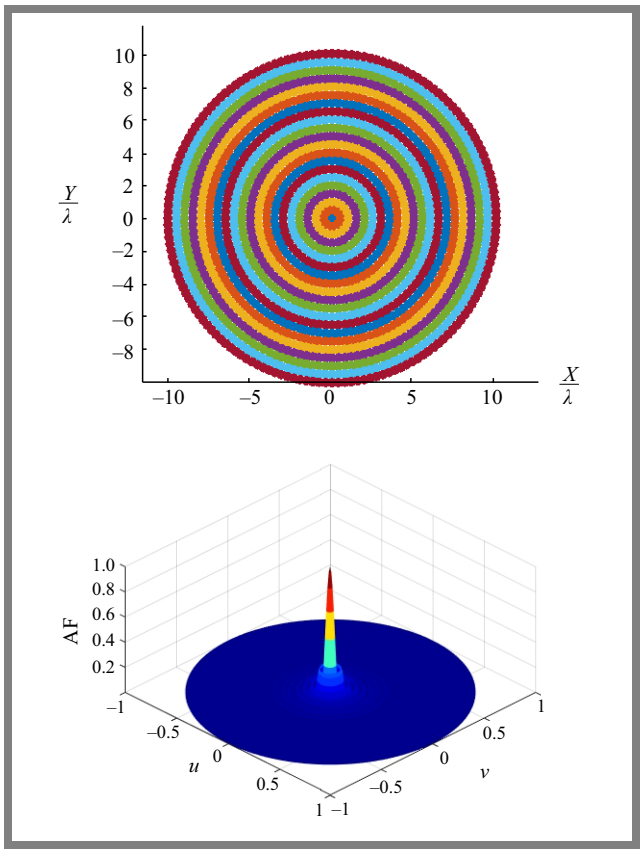

Fig. 8. Results for the proposed antenna for $C = 12$.

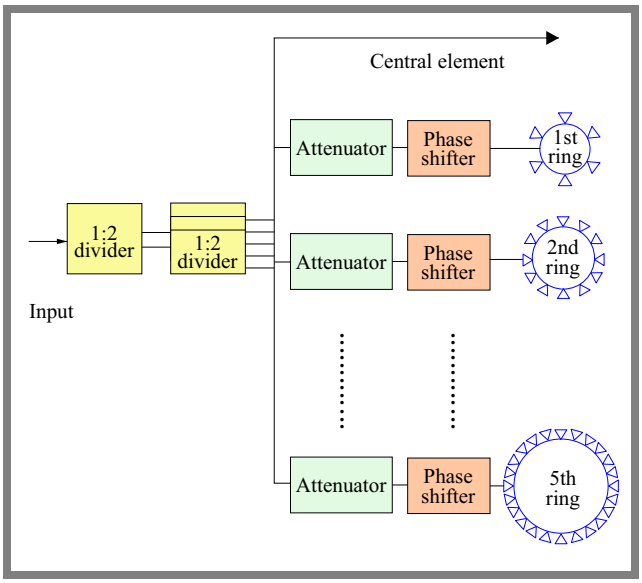

Fig. 9. Implementation of the proposed circular array with concentric subarray rings.

array are much better than in the case of the conventional circular array based on individual elements. This proves the effectiveness and practical applicability of the proposed array. The described idea may be expanded in future research to include multiple wireless power transmission receivers, with each receiver being at a different location, so that the optimizer maximizes the received powers over all of them.

References

[1] A. Massa, G. Oliveri, F. Viani, and P. Rocca, "Array Designs for Long-distance Wireless Power Transmission: State-of-the-art and Innovative Solutions", *Proceedings of the IEEE*, vol. 101, pp. 1464–1481, 2013 (https://doi.org/10.1109/JPROC.2013.2245491).

[2] R.H. Nansen, "Wireless Power Transmission: The Key to Solar Power Satellites", *IEEE Aerospace and Electronic Systems Magazine*, vol. 11, pp. 33–39, 1996 (https://doi.org/10.1109/62.484148).

[3] N. Shinohara, "Beam Control Technologies with a High-efficiency Phased Array for Microwave Power Transmission in Japan", *Proceedings of the IEEE*, vol. 101, pp. 1448–1463, 2013 (https://doi.org/10.1109/JPROC.2013.2253062).

[4] Y. Wang *et al.*, "Design of a Microwave Power Transmission Demonstration System for Space Solar Power Station", *International Journal of RF and Microwave Computer-Aided Engineering*, vol. 32, art. no. e23523, 2022 (https://doi.org/10.1002/mmce.23523).

[5] Y. Song *et al.*, "Research on the Multiobjective Optimization of Microwave Wireless Power Receiving in an Unmanned Aerial Vehicle Network", *Complexity*, vol. 2020, art. no. 8882528, 2020 (https://doi.org/10.1155/2020/8882528).

[6] G. Oliveri, L. Poli, and A. Massa, "Maximum Efficiency Beam Synthesis of Radiating Planar Arrays for Wireless Power Transmission", *IEEE Transactions on Antennas and Propagation*, vol. 61, pp. 2490–2499, 2013 (https://doi.org/10.1109/TAP.2013.2241714).

[7] J.R. Mohammed, "Synthesizing Non-uniformly Excited Antenna Arrays Using Tiled Subarray Blocks", *Journal of Telecommunications and Information Technology*, vol. 2023, pp. 25–29, 2023 (https://doi.org/10.26636/jtit.2023.4.1417).

[8] J.R. Mohammed and K.H. Sayidmarie, "Sensitivity of the Adaptive Nulling to Random Errors in Amplitude and Phase Excitations in Array Elements", *Journal of Telecommunication, Electronic and Computer Engineering*, vol. 10, pp. 51–56, 2018 (https://jtec.utem.edu.my/jtec/article/view/2023).

[9] J.R. Mohammed, "Beam-pattern Control via Thinned Elements Strategy in Linear and Planar Phased Arrays", *Progress In Electromagnetics Research Letters*, vol. 111, pp. 79–84, 2023 (https://doi.org/10.2528/PIERL23022403).

[10] A.J. Abdulqader, J.R. Mohammed, and A.A. Yaser, "A T-shaped Polyomino Subarray Design Method for Controlling Sidelobe Level", *Progress In Electromagnetics Research C*, vol. 126, pp. 243–251, 2022 (https://doi.org/10.2528/PIERC22080803).

[11] T. Isernia, M. D'Urso, and O.M. Bucci, "A Simple Idea for an Effective Sub-arraying of Large Planar Sources", *IEEE Antennas and Wireless Propagation Letters*, vol. 8, pp. 169–172, 2008 (https://doi.org/10.1109/LAWP.2008.2000943).

[12] J.R. Mohammed, "A Method for Thinning Useless Elements in the Planar Antenna Arrays", *Progress In Electromagnetics Research Letters*, vol. 97, pp. 105–113, 2021 (https://doi.org/10.2528/PIERL21022104).

[13] G. Oliveri and L. Poli, "Optimal Sub-arraying of Compromise Planar Arrays Through an Innovative ACO-weighted Procedure", *Progress In Electromagnetics Research*, vol. 109, pp. 279–299, 2010 (https://doi.org/10.2528/PIER10092008).

[14] J.R. Mohammed, "An Optimum Side-lobe Reduction Method with Weight Perturbation", *Journal of Computational Electronics*, vol. 18, pp. 705–711, 2019 (https://doi.org/10.1007/s10825-019-01323-5).

[15] J.R. Mohammed, R.H. Thaher, and A.J. Abdulkadeer, "Linear and Planar Array Pattern Nulling via Compressed Sensing", *Journal of Telecommunications and Information Technology*, vol. 2021, pp. 50–55, 2021 (https://doi.org/10.26636/jtit.2021.152921).

[16] L. Xun, D. Baoyan, and S. Liwei, "Design of Clustered Planar Arrays for Microwave Wireless Power Transmission", *IEEE Transactions on Antennas and Propagation*, vol. 67, pp. 606–611, 2019 (https://doi.org/10.1109/TAP.2018.2874670).

[17] P. Rocca, N. Anselmi, A. Polo, and A. Massa, "An Irregular Two-sizes Square Tiling Method for the Design of Isophoric Phased Arrays", *IEEE Transactions on Antennas and Propagation*, vol. 68, pp. 4437–4449, 2020 (https://doi.org/10.1109/TAP.2020.2970088).

[18] M. Salucci, G. Gottardi, N. Anselmi, and G. Oliveri, "Planar Thinned Array Design by Hybrid Analytical-stochastic Optimization", *IET Microwaves, Antennas and Propagation*, vol. 11, pp. 1841–1845, 2017 (https://doi.org/10.1049/iet-map.2017.0349).

[19] J.R. Mohammed, "Unconventional Method for Antenna Array Synthesizing Based on Ascending Clustered Rings", *Progress In Electromagnetics Research Letters*, vol. 117, pp. 69–73, 2024 (https://doi.org/10.2528/PIERL23122201).

[20] R. Vescovo and L. Pajewski, "Multiple-ring Circular Array for Ground-penetrating Radar Applications: Basic Ideas and Preliminary Results", *Journal of Telecommunications and Information Technology*, vol. 2017, pp. 25–29, 2017 (https://doi.org/10.26636/jtit.2017.120217).

[21] B. Yektakhah, A.M.H. Nasr, A.H. Mohamed, and K. Sarabandi, "Low-complexity Wideband Circularly Polarized Modular Scalable Phased Array for Vehicular Satellite Communication", *IEEE Open Journal of Antennas and Propagation*, vol. 6, pp. 854–863, 2025 (https://doi.org/10.1109/OJAP.2025.3551624).

[22] J.R. Mohammed, "Design of Printed Yagi Antenna with Additional Driven Element for WLAN Applications", Progress In Electromagnetics Research C, vol. 37, pp. 67–81, 2013 (https://doi.org/10.2528/PIERC12121201).

[23] M.M. Rahman *et al.*, "A Comprehensive Review of Wireless Power Transfer Methods, Applications, and Challenges", *Engineering Reports*, vol. 6, art. no. e12951, 2024 (https://doi.org/10.1002/eng2.12951).

[24] J.R. Mohammed, "Rectangular Grid Antennas with Various Boundary Square-rings Array", *Progress In Electromagnetics Research Letters*, vol. 96, pp. 27–36, 2021 (https://doi.org/10.2528/PIERL20112402).

[25] J.R. Mohammed, A.J. Abdulkadeer, and R.H. Thaher, "Array Pattern Recovery Under Amplitude Excitation Errors Using Clustered Elements", *Progress In Electromagnetics Research M*, vol. 98, pp. 183–192, 2020 (https://doi.org/10.2528/PIERM20101906).

[26] A.E.A. Blomberg, A. Austeng, and R.E. Hansen, "Adaptive Beamforming Applied to a Cylindrical Sonar Array Using an Interpolated Array Transformation", *IEEE Journal of Oceanic Engineering*, vol. 37, pp. 25–34, 2012 (https://doi.org/10.1109/JOE.2011.2169611).

[27] J.R. Mohammed, "Phased Sub-arrays Pattern Synthesis Method with Deep Sidelobe Reduction and Narrow Beamwidth", *IETE Journal of Research*, vol. 68, pp. 3130–3137, 2020 (https://doi.org/10.1080/03772063.2020.1853616).

[28] J.R. Mohammed, A.J. Abdulkadeer, and R.H. Thaher, "Antenna Pattern Optimization via Clustered Arrays", *Progress In Electromagnetics Research M*, vol. 95, pp. 177–187, 2020 (https://doi.org/10.2528/PIERM20042307).

[29] J.R. Mohammed, "Simplified Rectangular Planar Array with Circular Boundary for Side Lobe Suppression", *Progress In Electromagnetics Research M*, vol. 97, pp. 57–68, 2020 (https://doi.org/10.2528/PIERM20062906).

[30] A.J. Abdulqader, J.R. Mohammed, and Y.E.M. Ali, "Beam Pattern Optimization via Unequal Ascending Clusters", *Journal of Telecommunications and Information Technology*, vol. 2023, pp. 1–7, 2023 (https://doi.org/10.26636/jtit.2023.168523).

[31] Q. Shi, Z. Zheng, and Y. Sun, "Pattern Synthesis of Subarrayed Large Linear and Planar Arrays Using K-means Solution", *IEEE Antennas and Wireless Propagation Letters*, vol. 20, pp. 693–697, 2021 (https://doi.org/10.1109/LAWP.2021.3060190).

Jafar Ramadhan Mohammed, Professor
College of Electronics Engineering
https://orcid.org/0000-0002-8278-6013
E-mail: jafar.mohammed@uoninevah.edu.iq
Ninevah University, Mosul, Iraq
https://uoninevah.edu.iq